Asian Journal of Chemistry; Vol. 37, No. 11 (2025), 2661-2667
ASIAN JOURNAL OF CHEMISTRY
https://doi.org/10.14233/ajchem.2025.34551

Novel Bischalcones and their Heterocyclic Derivatives as Strong Inhibitors of the MurE Enzyme: Synthesis, Biological Assessment and Molecular Docking Studies

G. BUELA PRIYANKA[1,2,*] and GIRIJA SASTRY VEDULA[1]

[1]Department of Pharmaceutical Chemistry, Andhra University College of Pharmaceutical Sciences, Andhra University, Visakhapatnam-530003, India
[2]School of Pharmacy, Guru Nanak Institutions Technical Campus (Autonomous), Ibrahimpatnam-501506, India

*Corresponding author: E-mail: priyankabuela@gmail.com

Received: 28 July 2025 *Accepted*: 6 September 2025 *Published online*: 27 October 2025 AJC-22152

A series of novel 2,6-*bis*((*E*)-benzylidene)-4-methylcyclohexan-1-one derivatives were synthesized at room temperature over 18-48 h by reacting aromatic and heterocyclic aldehydes with alkyl-substituted cyclic ketones, using alcohol as solvent and a base as catalyst. The successful formation of these novel heterocycle-containing bischalcones was confirmed through spectral characterization techniques. The Alamar Blue Assay (MABA) method was used to perform the biological evaluation for antitubercular activity and the compounds showed promise as powerful and innovative inhibitors for the development of new antitubercular therapies. Furthermore, compounds **3a**, **3b**, **3c**, **3g**, **3i**, **3k** and **3l** exhibit high binding energies with the target protein Mur E enzyme of the Mur pathway, molecular docking verified the uncompetitive inhibition of *M. tuberculosis* Mur E enzyme.

Keywords: Bischalcone, Cyclicketone, Mur E enzyme, Antitubercular activity, Molecular docking studies.

INTRODUCTION

Tuberculosis (TB) remains one of the most significant threats to global health. More than 10.8 million people continue to fall ill with TB every year and the number has been rising since 2021. In 2024, approximately 10.8 million new TB cases were estimated and about 1.25 million people died from the disease, including 161,000 HIV-positive individuals [1,2]. Among these, women constituted a large share of morbidity and mortality, highlighting that TB is one of the top causes of death among women worldwide [3-5]. Regionally, the burden was disproportionately high in South-East Asia (~29%), Africa (~27%) and the Western Pacific (~19%) regions. India alone contributed about 26% of the global TB caseload, with China accounting for another ~12% [6].

The causative pathogen *Mycobacterium tuberculosis* is transmitted through airborne droplets and has evolved sophisticated strategies to evade the host immune response, allowing it to persist within macrophages for extended periods [7-9]. Once host defenses are breached, the bacteria can establish latent infection or re-activate, causing active disease. Since drug resistance is an escalating problem, discovering novel therapeutic targets that work against both drug-sensitive and resistant strains is of high urgency. One promising area is the Mur pathway, which is essential for peptidoglycan biosynthesis in bacteria. The cytoplasmic steps of this pathway especially the early steps catalyzed by MurA and MurB (leading to UDP-N-acetylmuramoyl precursors) and the subsequent addition of amino acids by MurC, MurD, MurE and MurF ligases are highly conserved and essential [10-12]. MurA catalyzes the transfer of an enolpyruvate moiety from phosphoenolpyruvate (PEP) to UDP-N-acetylglucosamine, forming the UDP-N-acetylmuramate enol intermediate, which MurB then reduces to yield UDP-N-acetylmuramate [13,14]. The pathway then proceeds through the sequential ligation of amino acids: MurC attaches L-alanine, MurD adds D-glutamine, MurE incorporates L-lysine (or *meso*-diaminopimelate in several bacteria) and finally MurF adds the dipeptide D-Ala-D-Ala, all ATP-dependent steps [15,16].

Bischalcones are well-known organic compounds exhibiting a broad spectrum of biological activities, including anti-inflammatory, antimicrobial [17,18], antitubercular [19], antioxidant [20,21], antiviral [22], antibacterial [23,24], antifungal [18], anticancer [25-27], antimalarial [28] and anti-neurode-

generative effects [29]. Moreover, bischalcones are also recognized as highly active intermediates, playing a pivotal role in the synthesis of various biologically active heterocyclic derivatives too [30].

In light of these properties, we designed and synthesized novel molecules integrating two chalcone pharmacophores within a single framework. This hybridization strategy aims to enhance the biological efficacy of the compounds, potentially providing new candidates for the treatment of diverse diseases [31]. Given the urgent global health threat posed by tuberculosis (TB), particularly in the context of multidrug-resistant (MDR) and extensively drug-resistant (XDR) strains of *Mycobacterium tuberculosis*, the development of novel chemotypes is critical. Bischalcones, with their reported antitubercular activity and potential for further functionalization, offer a promising scaffold for the design of TB-targeted agents. Their ability to interfere with key bacterial pathways, such as cell wall biosynthesis and enzyme inhibition, makes them compelling candidates in the ongoing search for more effective TB therapeutics.

EXPERIMENTAL

All chemicals and reagents used in this study were procured from Mumbai Research Labs and utilized without further purification unless otherwise stated. The melting points of the synthesized compounds were determined using a Remi electronic melting point apparatus and are reported uncorrected. Thin-layer chromatography (TLC) was performed on precoated Merck aluminum silica gel 60 F_{254} plates with a thickness of 0.5 mm to monitor reaction progress and assess the purity of the synthesized compounds. Infrared (IR) spectra were recorded on an Agilent FTIR spectrometer using the KBr pellet technique. Proton nuclear magnetic resonance (^{1}H NMR) spectra were obtained on a VARIAN NMR spectrometer operating at 500 MHz.

Synthesis of 2,6-*bis*(E)-benzylidene-4- methylcyclohexanone derivatives: A mixture of aldehyde (2 mol) and methylcyclohexanone (1 mol) was mixed with 40 mL of absolute ethanol and sodium hydroxide solution, then heated for 14 to 48 h. Once after the completion of reaction, the reaction mixture was cooled and neutralized by using HCl as acid. This resulted in the formation of a precipitate, which was collected by filtration, washed with cold water and dried (**Scheme-I**). The crude product was recrystallized from ethanol to afford the colored pure compounds.

2*E*,6*E*-*bis*(3-Phenylallylidene)-4-methylcyclohexan-1-one (3a): Dark yellow powder, yield: 88%, m.p.: 236-238 ºC; ^{1}H NMR (500 MHz, $CHCl_3$-d_6) δ ppm: 1.19 (d, 3H), 2.01 (t, 2H), 2.32 (t, 4H), 6.98 (dd, 2H), 7.02 (t, 4H), 7.20-7.54 (m, 10H). ^{13}C NMR (125 MHz, $CHCl_3$-d_6) ppm: 21.67, 28.44, 34.80, 38.0, 38.1, 38.2, 123.2, 123.70, 125.2, 125.3, 127.9, 127.9, 128.5, 128.5, 128.6, 128.6, 128.7, 128.7, 135.2, 136.79, 138.4, 138.6, 140.80, 147.9, 148.2, 188.75. HRMS: *m/z* for $C_{25}H_{24}O$ $[M+H]^+$: 341.19, found: 341.19.

2*E*,6*E*-*bis*(2,4-Dichlorobenzylidene)-4-methylcyclohexan-1-one (3b): Pale yellow powder, yield: 72%, m.p.: 230-235 ºC; ^{1}H NMR (500 MHz, $CHCl_3$-d_6) δ ppm: 1.04 ppm (t, 3H), 1.80(2H), 2.38-2.67(4H, t), 7.26-7.36 (2H, s), 7.39-7.74 (8H, m); ^{13}C NMR (125 MHz, $CHCl_3$-d_6) ppm: 21.67, 28.44, 34.80, 34.82, 23.70, 123.72, 126.8, 126.9, 128.9, 128.9, 130.3, 130.3, 131.2, 131.2, 136.79, 136.78, 137.1, 137.1, 140.80, 140.90, 188.75. HRMS: *m/z* for $C_{21}H_{16}Cl_4O$ $[M + H]^+$: 426.16, found: 426.16.

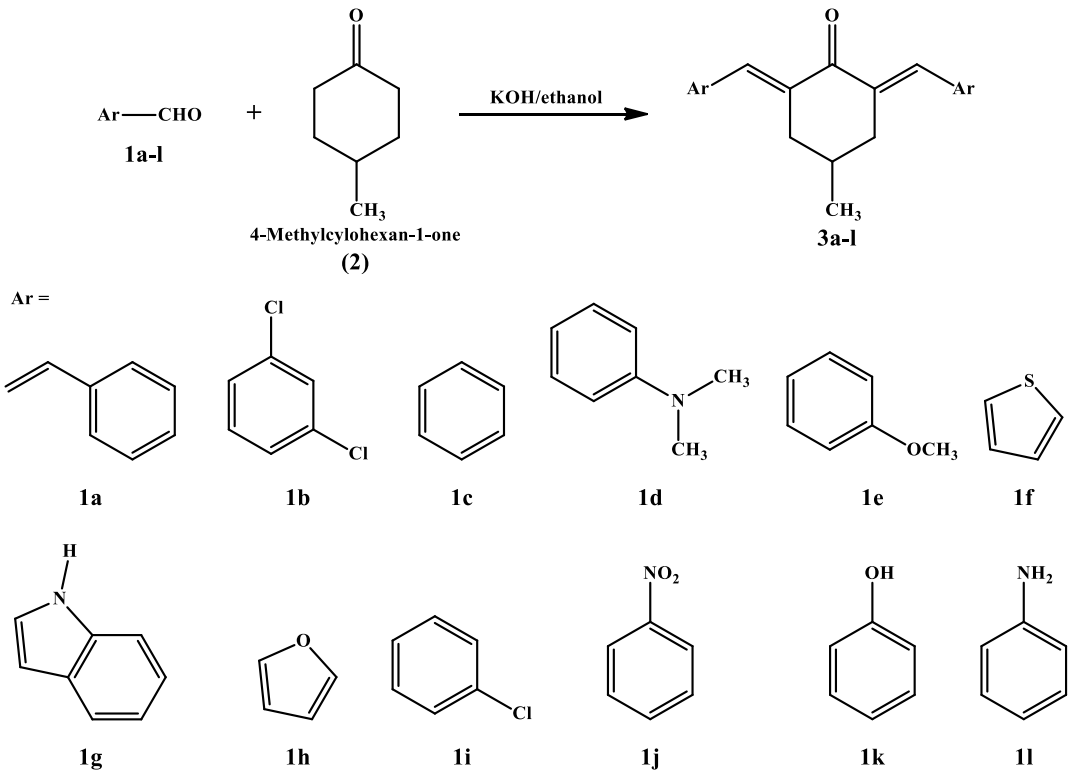

Scheme-I: Synthesis of (2E,6E)-2,6-diethylidene-4-methylcyclohexan-1-one derivatives

2*E*,6*E*-*Bis*(benzylidene)-4-methylcyclohexan-1-one (3c): Pale yellow powder, yield: 71%, m.p.: 258 ºC, ^{1}H NMR (500 MHz, $CHCl_3$-d_6) δ ppm: 1.83 (t, 3H), 2.50 (2H), 2.60-3.53 (4H), 7.38 (2H), 7.49-7.84 (8H, m); ^{13}C NMR (125 MHz $CHCl_3$-d_6) ppm: 21.3, 36.5, 37.5, 37.8, 127.6, 127.6, 128.5, 128.5, 128.53, 128.5, 128.6, 128.6, 128.6, 128.6, 132.2, 132.2, 135.2, 135.2, 137.1, 137.1, 190.4. HRMS: *m/z* for $C_{21}H_{20}O$ $[M+H]^+$: 289.15, found: 289.15.

2*E*,6*E*-*bis*(4-(Dimethylamino)benzylidene)-4-methylcyclohexan-1-one (3d): Dark orange powder, yield: 82%, m.p.: 322 ºC; ^{1}H NMR (500 MHz, $CHCl_3$-d_6) δ ppm: 1.06 ppm (d, 3H), 1.60 (d, 2H), 2.50 (s, 4H), 2.98 (s, 12 H), 6.76 (d, 4H), 7.40 (d, 2H), 7.54, (d, 4H). ^{13}C NMR (125 MHz, $CHCl_3$-d_6) δ ppm: 21.67, 37.44, 37.80, 37.80, 41.3, 41.3, 41.3, 41.3, 111.7, 111.7, 111.7, 111.7, 124.70, 124.70, 129.7, 129.7, 129.7, 129.7, 132.2, 132.2, 137.79, 137.79, 150.3, 150.3, 188.75. HRMS: *m/z* for $C_{25}H_{30}N_2O$ $[M + H]^+$: 375.24, found: 375.14.

2*E*,6*E*-*bis*(4-Methoxybenzylidene)-4-methylcyclohexan-1-one (3e): Pale yellow substance, yield: 75%, m.p.: 266 ºC. ^{1}H NMR (500 MHz, $CHCl_3$-d_6) δ ppm: 1.03 (t, 3H), 1.81 (s, 2H), 2.56 (t, 2 H), 2.95 (d, 2H), 3.35 (s, 6H), 7.02 (d, 2H), 7.26 (2H), 7.37, (2H), 7.50 (d, 2H), 7.59 (s, 2H); ^{13}C NMR (125 MHz, $CHCl_3$-d_6) δ ppm: 21.67, 27.44, 34.80, 37.8, 55.8, 55.8, 114.2, 114.2, 114.3, 114.3, 123.70, 123.71, 127.5, 127.5, 130.2, 130.2, 130.2, 130.2, 132.2, 132.2, 136.79, 136.79, 159.80, 159.80, 188.75. HRMS: *m/z* for $C_{23}H_{24}O_3$ $[M + H]^+$: 349.18, found: 349.16.

2*E*,6*E*-*bis*(Thiophene-2ylmethylene)-4-methylcyclohexan-1-one (3f): Yellow powder, yield: 86%, m.p.: 342 ºC. ^{1}H NMR (500 MHz, $CHCl_3$-d_6) δ ppm: 1.19 (d, 3H), 1.63 (s, 2H), 2.03 (s, 2H), 2.48-2.55 (t, 2H), 6.53 (s, 2H), 6.69 (s, 2H), 7.2 (s, 2H), 7.56 (d, 2H). ^{13}C NMR 125 MHz, $CHCl_3$-d_6) ppm: 21.68, 28.45, 34.81, 124.70-136.78, 140.81, 188.76. HRMS: *m/z* for $C_{17}H_{16}S_2O$ $[M + H]^+$: 301.06, found: 301.16.

2*E*,6*E*-*bis*(1*H*-indol-3-yl)-4-methylcyclohexan-1-one (3g): Brown fine powder, yield: 85%, m.p.: 336 ºC. ^{1}H NMR (500 MHz, $CHCl_3$-d_6) δ ppm: 1.08 (d, 3H), 1.66 (s, 2H), 2.09-2.50 (s, 2H), 3.63 (s, 2H), 7.22-7.28 (t, 4 H), 7.50 (d, 2H), 8.08 (d, 2H), 8.28 (d, 2H), 9.94 (s, 2H), 12.13 (s, 2H). ^{13}C NMR 125 MHz, $CHCl_3$-d_6) δ ppm: 21.67, 28.44, 34.80, 123.70, 136.79, 140.80, 188.75. HRMS: *m/z* for $C_{25}H_{22}N_2O$ $[M + H]^+$: 367.18; found 367.18.

2*E*,6*E*-*bis*(Furan-2-ylmethylene)-4-methylcyclohexan-1-one (3h): Orange powder, yield: 84%, m.p.: 354 ºC. ^{1}H NMR (500 MHz, $CHCl_3$-d_6) δ ppm: 1.10, (s, 3H), 2.50 (s, 2H), 3.34-3.38 (s, 4H), 6.70 (s, 2H), 6.96 (s, 2H), 7.40 (s, 2H), 7.93 (s, 2H); ^{13}C NMR (125 MHz, $CHCl_3$-d_6) δ ppm: 21.69, 28.46, 34.82, 124.70-136.78, 140.82, 188.76 ppm. HRMS: *m/z* for $C_{17}H_{16}O_3$ $[M + H]^+$: 269.11, found: 269.11.

2*E*,6*E*-*bis*(4-Chlorobenzylidene)-4-methylcyclohexan-1-one (3i): Light yellow powder, yield: 72%, m.p.: 291-294 ºC.^{1}H NMR (500 MHz, $CHCl_3$-d_6) δ ppm: 1.08, (s, 3H), 1.66 (s, 2H), 2.10 (s, 4H), 7.38 (s, 2H), 7.62 (s, 2H), 7.63 (s, 2H), 7.68 (s, 2H), 7.68 (s, 2H). ^{13}C NMR (125 MHz, $CHCl_3$-d_6) δ ppm: 21.26, 37.56, 38.52, 38.54, 128.72, 128.75, 128.82, 128.85, 129.37, 129.37, 129.58, 129.59, 132.25, 132.28, 133.32, 133.34, 133.52, 133.53, 137.12, 137.12, 190.48. HRMS: *m/z* for $C_{21}H_{18}Cl_2O$ $[M + H]^+$: 358.07, found: 358.07.

2*E*,6*E*-*bis*(2-nitrobenzylidene)cyclohexan-1-one (3j): Light yellow powder, yield: 72%, m.p.: 291-294ºC. ^{1}H NMR (500 MHz, $CHCl_3$-d_6) δ ppm: 1.08, (s, 3H), 1.66 9 (s, 2H), 2.01 (s, 4H), 7.78 (s, 2H), 7.96 (s, 2H), 7.98 (s, 2H), 8.03 (s, 2H), 8.28 (s, 2H). ^{13}C NMR 125 MHz, $CHCl_3$-d_6) δ ppm: 21.26, 37.46, 38.52, 38.84, 123.82, 123.85, 127.35, 127.35, 127.37, 127.37, 128.79, 134.12, 134.18, 137.12, 137.14, 145.02, 145.03, 147.52, 147.66, 190.28. HRMS: *m/z* for $C_{21}H_{18}N_2O_5$ $[M+H]^+$: 379.12, found: 379.14.

2*E*,6*E*-*bis*(2-Hydroxybenzylidene)-4-methylcyclohexan-1-one (3k): Light yellow powder, yield 79%, m.p.: 291-294 ºC. ^{1}H NMR (500 MHz, $CHCl_3$-d_6) ppm: 1.08, (s, 3H), 1.66 (s, 2H), 2.01 (s, 2H), 6.78 (s, 2H), 6.86 (s, 2H), 7.08 (s, 2H), 7.63 (s, 2H), 10.28 (s, 2H). ^{13}C NMR 125 MHz, $CHCl_3$-d_6) δ ppm: 21.26, 37.46, 38.52, 38.84, 116.40, 116.82, 118.68, 118.62, 124.70, 124.78, 128.78, 128.79, 137.12, 137.18, 144.02, 144.03, 145.52, 145.66, 190.28. HRMS: *m/z* for $C_{21}H_{20}O_3$ $[M+H]^+$: 321.14, found: 321.14.

2,6-*bis*(*E*)-2-Aminobenzylidene)-4-methylcyclohexan-1-one (3l): Light yellow powder, yield: 75%, m.p.: 291-294 ºC.^{1}H NMR (500 MHz, $CHCl_3$-d_6) ppm: 1.18, (s, 3H), 1.63 (s, 2H), 2.04 (s, 4H), 5.02 (s, 2H), 6.58 (s, 2 H), 6.78 (s, 2H), 6.86 (s, 2H), 7.40 (s, 2H), 7.93 (s, 2H). ^{13}C NMR (125 MHz, $CHCl_3$-d_6) δ ppm: 21.26, 37.46, 38.52, 38.84, 116.40, 116.82, 118.68, 118.62, 124.70, 124.78, 128.78, 128.79, 137.12, 137.18, 144.02, 144.03, 145.52, 145.66, 190.28. HRMS: *m/z* for $C_{21}H_{22}N_2O$ ($[M+H]^+$): 319.18.11, found: 319.18.

Molecular docking: From the molecular docking studies, identification of the novel antitubercular drugs was done by analyzing the molecular interactions between the ligands and the Mur E receptor protein. For molecular docking, the target proteinsare selected based on the several criteria, which should possess the resolution between 2.0-3.0 Å and its structure was identified by X-ray diffraction method, must contain co-crystallized ligand and the selected protein's 3D structure must show no breaks in its structure. The Mur E receptor protein has recently emerged as a promising target for the development of antitubercular drugs featuring *bis*chalcone nucleus [12]. The Mur E receptor protein crystal structure was obtained from Protein Data Bank (PDB ID: 2XJA), which has the resolution of 3.0 Å. The interactions between the designed 3D-structured *bis*chalcones and the active site of the 2XJA was analyzed by using Auto Dock 4.2.6 software [32]. To draw the designed structures, ChemSketch version 2022.1.2 from ACD/Labs was utilized which were then converted into the suitable 3D models. Using molecular mechanics, energy minimization was underwent of these models, preparing them for the molecular docking and the corresponding PDB files are created. The aim of the docking studies is to identify potential binding locations for the ligands within the receptors active site. By using default parameters, Grid-based docking studies were performed, with UDP-N-acetyl muramoyl-L-alanyl-D-glutamate-2,6-diaminopimelate ligase used as reference ligands at the Mur E active site.

RESULTS AND DISCUSSION

A series of novel *bis*chalcone derivatives were synthesized through condensation reactions involving various aromatic and heterocyclic aldehydes, following established synthetic protocols. The resulting compounds were characterized using

spectroscopic techniques, including NMR, IR and mass spectrometry. These derivatives were subsequently evaluated for their potential antitubercular activity. Molecular docking studies at the Mur E receptor protein active site region gives the data of binding energies (kcal/mol), hydrogen bond length, number of hydrogen bonds and interacted amino acid residues, shown in Table-1. In comparison to the reference ligand that is UDP-N-acetyl muramoyl-L-alanyl-D-glutamate-2,6-diaminopimelate ligase with the binding energy of -0.25 kcal/mol. Compounds **3b** and **3l** exhibited the highest binding energies of -0.8 kcal/mol and -7.8 kcal/mol at the active site of Mur E receptor protein. Figs. 1-6 depicts the 2D structures of Mur E receptor protein and the binding mode of UDP-N-acetyl muramoyl-L-alanyl-D-glutamate-2,6-diaminopimelate ligase and the compounds **3a**-**3l** at the active site region of the Mue E protein (PDB ID:2XJA).

For the target 2XJA, the best-performing compounds are compound **3b**, which has the highest docking score of -8.02, indicating the strongest binding among all hybrids. This is followed by compound **3l**, with a score of -7.80 (Fig. 1).

TABLE-1
BINDING ENERGIES, H-BOND INTERACTIONS AND INHIBITORY PROFILES OF COMPOUNDS **3a-l** AND REFERENCE

Compound name	Binding energies	Inhibitory concentration	H-Bond interactions	Amino acid residues	Hydrogen bond length
3a	-7.50	3.19 µM	0	No	–
3b	-8.02	1.31 µM	1	ARG128	3.08
3c	-7.37	3.94 µM	0	No	–
3d	-6.72	11.84 µM	0	No	–
3e	-6.75	11.37 µM	0	No	–
3f	-6.92	8.53 µM	1	ARG128	5.32
3g	-7.79	1.94 µM	1	ARG128	5.02
3h	-6.47	18.04 µM	0	No	–
3i	-7.62	2.58 µM	1	ARG128	3.54
3j	-6.75	11.27 µM	3	ARG128, ARG230	2.65, 2.74, 3.01
3k	-7.67	2.39 µM	1	ARG128	2.59
3l	-7.80	1.92 µM	1	ARG128	5.02
Reference	-3.25	650.64 mM	4	LEU67, SER84, THR85, ARG128	3.17, 2.84, 2.73, 2.66

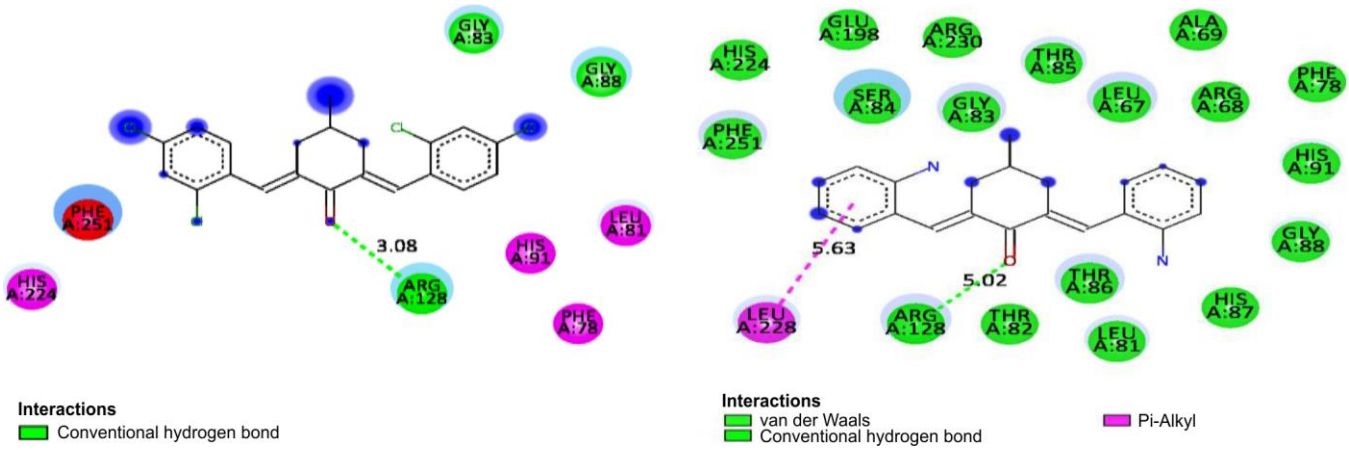

Fig. 1. Interaction of compounds **3b**, **3l** at target protein 2XJA

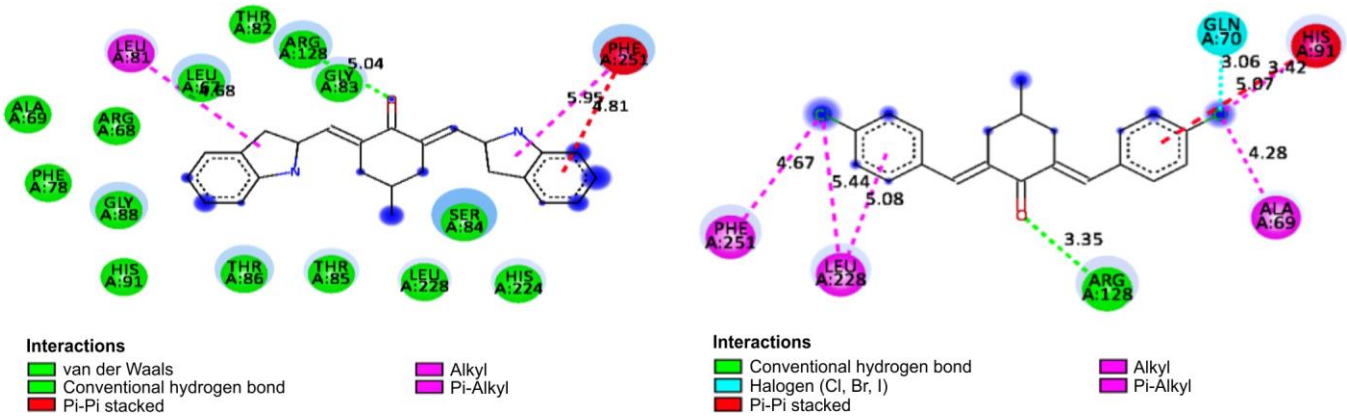

Fig. 2. Interaction of compounds **3g**, **3k** at target protein 2XJA

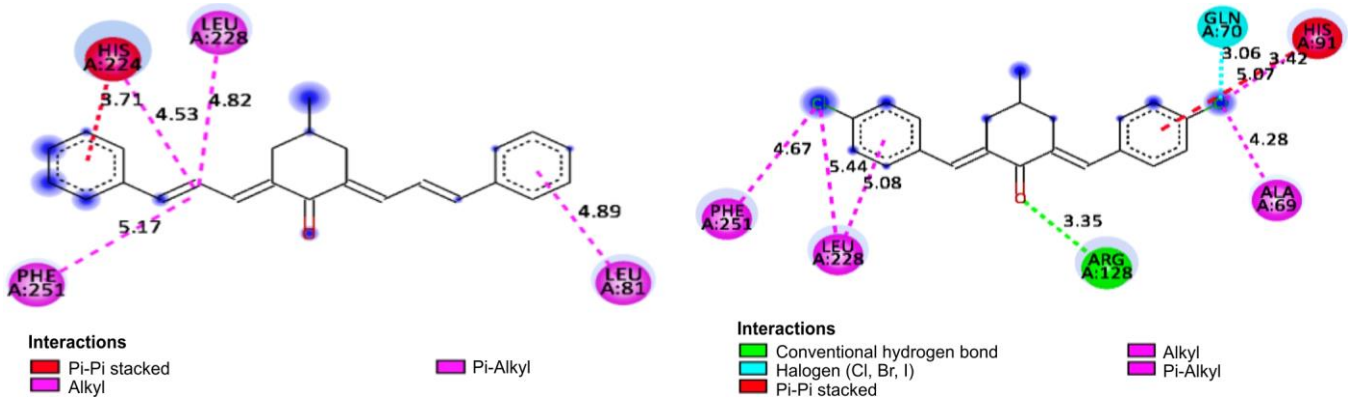

Fig. 3. Interaction of compounds **3a**, **3i** at target protein 2XJA

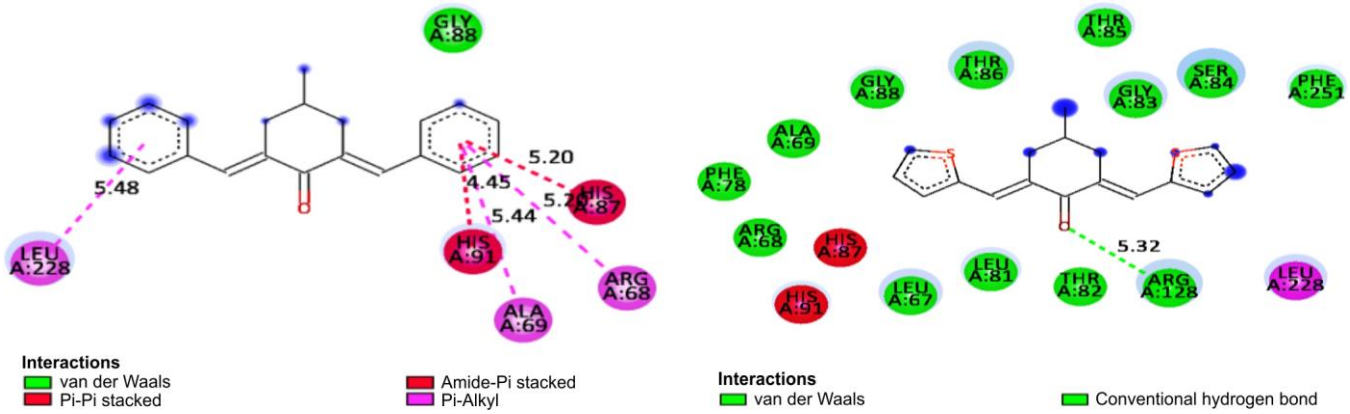

Fig. 4. Interaction of compounds **3c**, **3f** at target protein 2XJA

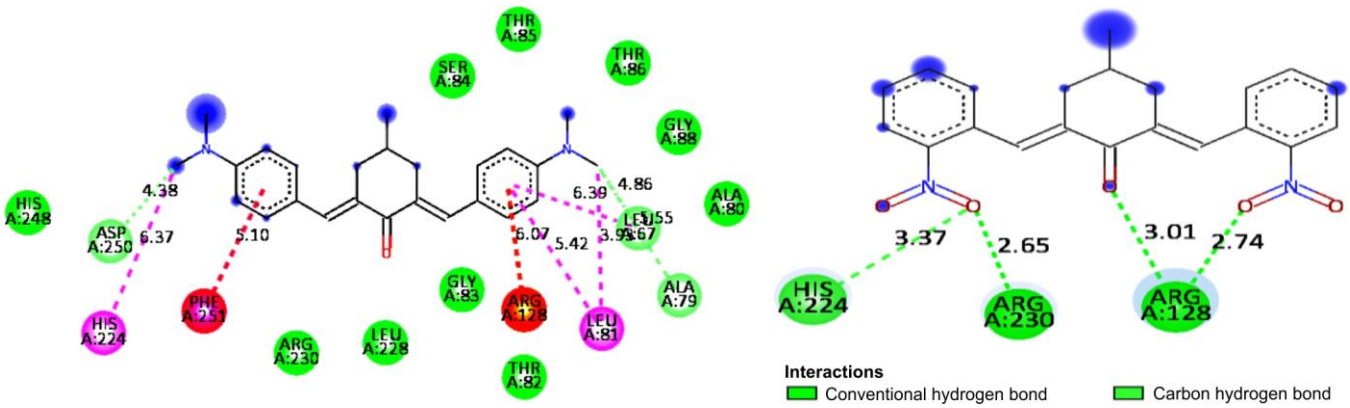

Fig. 5. Interaction of compounds **3e**, **3j** at target protein 2XJA

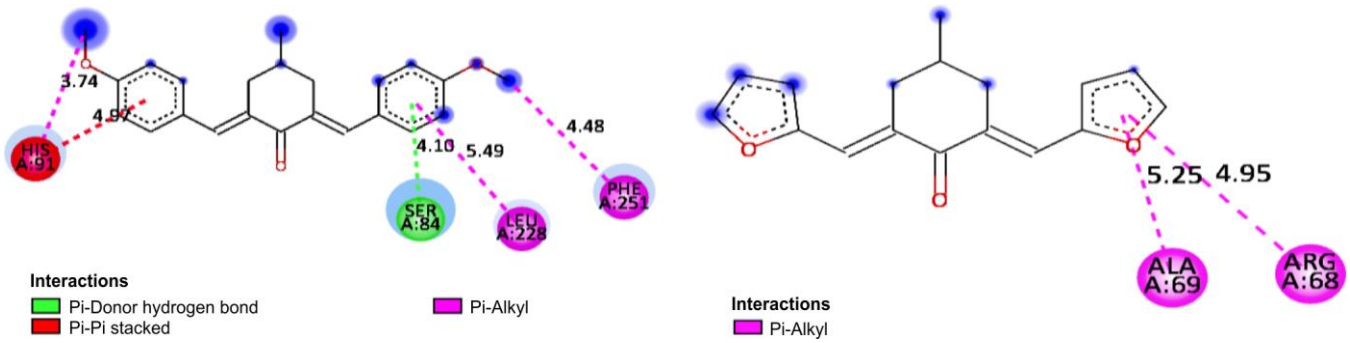

Fig. 6. Interaction of compounds **3d**, **3h** at target protein 2XJA

These results suggest that the electron-withdrawing groups such as chlorine (-Cl) and electron-donating groups, like amino (-NH_2), significantly enhance binding affinity to this target. Moreover, compounds **3g** and **3k** have scores of -7.79 and -7.67, respectively (Fig. 2). This indicates that substituents at *para* positions of the phenyl ring, particularly electron donating groups such as hydroxyl (-OH) and heterocyclic substituents, also exhibit efficient binding to the target. Other compounds such as compounds **3a** and **3i**, also demonstrate good binding with scores of -7.50 and -7.67, respectively (Fig. 3) with groups like conjugated double bond and chlorine at *meta* position of phenyl ring exhibiting good binding scores with the target. Compounds **3c** and **3f** show the binding scores of -7.37 and -6.92 (Fig. 4) with phenyl ring and thiophene rings as substituents shows efficient binding scores. Other compounds **3e** and **3j** also shows similar scores of -6.75 (Fig. 5) with (–$N(CH_3)_2$) and the NO_2 groups at *meta* and *para* positions of phenyl ring is likely due to their ability to form the hydrogen bonds or electrostatic interactions with the target proteins, as demonstrated by compound **3j**. At last, compounds **3d** and **3h** show good binding scores of 6.72 and 6.47, respectively (Fig. 6) with (–OCH_3) at *meta* position of phenyl ring and furan ring as a substituent.

Anti-TB activity assessed by Alamar blue assay: On Lowenstein Jensen (LJ) medium the growth was suspended in the sterilized Middle brook 7H9 broth media, supplemented with glycerol (0.2%) and OADC-oleate-albumin-dextrose catalase (10%) enrichment. A dilution of 1:20 of this suspension was utilized as the inoculum for this method. The entire process was performed in the suitable safety hoods. Then 200 µL of sterile deionized water was added to minimize medium evaporation during incubation, to the outer perimeter wells of a sterile 96-well plate and compound serial dilutions were made directly on the plate and each well of the plate received 100 µL of the Middlebrook 7H9 broth. Then the final concentrations of the drug tested were 25, 12.5, 6.25, 3.125, 1.56 and 0.78 µg/ml. The plates were covered and then sealed with parafilm and incubated for five days at 37 ºC and to the each well 25 µL 1:1 mixture of alamar blue reagent and 10% of Tween 80. Later the plates were further incubated for 24 h more shows the signified blue well indicating no growth of bacteria, whereas the pink well scored as indication of bacterial growth. And the minimum inhibitory concentration was defined as the lowest concentration of the drug that prevents the colour change from blue to pink.

Halogen-substituted derivatives were analyzed, revealing that the *meta*-chloro derivative (**3b**) exhibited higher potency (IC_{50} = 1.31 µM) compared to the *para*-chloro derivative (**3i**), which had an IC_{50} of 2.58 µM. Compounds **3g** and **3l** showed strong antitubercular activity with the IC_{50} values of 1.94 and 1.92 µM. Hydroxy substituted compound **3k** (2-OH) demonstrated an IC_{50} of 2.39 µM. The high activity of these compounds is due to the ability of hydroxyl groups to form the hydrogen bonds with target. In contrast, the methoxy derivative (**3d**) displayed an IC_{50} of 11.84 µM, while the dimethylamino derivatives had an IC_{50} of 11.37 µM. The least active nitro derivatives were **3j** and **3h**, with the IC_{50} values of 11.27 µM and 18.04 µM. According to the structure-activity relationship (SAR) analysis, substances with certain substitutions such as chloro (-Cl), amino (-NH_2) and *meta*-methoxy (-OCH_3) groups, consistently displayed strong antitubercular activity along with favourable selectivity. Furthermore, compounds **3i** (IC_{50} = 2.58 µM), **3a** (IC_{50} = 3.19 µM), **3c** (IC_{50} = 3.94 µM), **3f** (IC_{50} = 8.53 µM) and **3h** (IC_{50} = 11.84 µM) were particularly effective against tubercular cells while demonstrating binding affinity to target proteins.

Conclusion

A series of novel *bis*chalcone hybrids were synthesized by reacting benzaldehyde derivatives with methyl cyclohexanone in the presence of ethanol as solvent and NaOH used as base. The reaction was carried out with continuous stirring for 18 to 48 h. The resulting products were recrystallized using ethanol. The targeted derivatives were analyzed using spectroscopic techniques like, ^{1}H NMR, ^{13}C NMR and mass and infrared spectroscopy. The outcomes were compared to a reference standard, rifampicin. All substances demonstrated significant anti-tubercular effects. The structure-activity relationship (SAR) elucidation indicated that the position of the substituents and their electron-donating or withdrawing properties play a crucial role in determining antitubercular activity. Notably, compounds **3a**, **3b**, **3f**, **3g** and **3h** exhibited stronger activity against *M. tuberculosis*. and the molecular docking studies were performed against the target Mur E receptor protein. Further research on their structural and molecular aspects is needed to better understand the specific way in which the compounds work and to develop these compounds as potential leads for the treatment of tuberculosis.

ACKNOWLEDGEMENTS

The authors are grateful to the Department of Pharmaceutical Chemistry, Andhra University, Vishakhapatnam, India, for providing the critical support in completing the current work.

CONFLICT OF INTEREST

The authors declare that there is no conflict of interests regarding the publication of this article.

REFERENCES

1. https://www.who.int/teams/global-programme-on-tuberculosis-and-lung-health/tb-reports/global-tuberculosis-report-2024
2. D. Goletti, G. Meintjes, B.B. Andrade, A. Zumla and S.S. Lee, *Int. J. Infect. Dis.*, **150**, 107325 (2025); https://doi.org/10.1016/j.ijid.2024.107325
3. S.M. Riaz, L. Sviland, K. Hanevik and T. Mustafa, *J. Infect. Public Health*, **17**, 102563 (2024); https://doi.org/10.1016/j.jiph.2024.102563
4. J. Samal, *Egypt. J. Bronchol.*, **19**, 24 (2025); https://doi.org/10.1186/s43168-025-00383-5
5. H. Lv, L. Wang, X. Zhang, C. Dang, F. Liu, X. Zhang, J. Bai, S. You, H. Chen, W. Zhang and Y. Xu, *Infect. Dis. Poverty*, **13**, 70 (2024); https://doi.org/10.1186/s40249-024-01247-8
6. T.Z. Malik, F. Ahmed, S. Roy, R. Agarwalla and R. Pathak, *Clin. Epidemiol. Global Health*, **34**, 102075 (2025); https://doi.org/10.1016/j.cegh.2025.102075

7. S. Abbasnia, A.M.H. Asnaashari, H. Sharebiani, S. Soleimanpour, A. Mosavat and S.A. Rezaee, *J. Clin. Tuberculosis Other Mycobact. Dis*., **36**, 100458 (2024); https://doi.org/10.1016/j.jctube.2024.100458
8. N. Mohammadnabi, J. Shamseddin, M. Emadi, A.B. Bodaghi, M. Varseh, A. Shariati, M. Rezaei, M. Dastranj and A. Farahani, *J. Clin. Lab. Anal*., **38**, e25122 (2024); https://doi.org/10.1002/jcla.25122
9. P. Chandra, S.J. Grigsby and J.A. Philips, *Nat. Rev. Microbiol.*, **20**, 750 (2022); https://doi.org/10.1038/s41579-022-00763-4
10. K. Eniyan, J. Rani, S. Ramachandran, R. Bhat, I.A. Khan and U. Bajpai, *SLAS Discov*., **25**, 70 (2020); https://doi.org/10.1177/2472555219881148
11. C. Paradis-Bleau, A. Lloyd, F. Sanschagrin, T. Clarke, A. Blewett, T.D.H. Bugg and R.C. Levesque, *BMC Biochem.*, **9**, 33 (2008); https://doi.org/10.1186/1471-2091-9-33
12. K. Mehta, M. Khambete, A. Abhyankar and A. Omri, *Pharmaceuticals* **16**, 377 (2023); https://doi.org/10.3390/ph16030377
13. J. Rani, Y. Silla, K. Borah, S. Ramachandran and U. Bajpai, *J. Biomol. Struct. Dyn.*, **38**, 2521 (2020); https://doi.org/10.1080/07391102.2019.1637280
14. A. El Zoeiby, F. Sanschagrin and R.C. Levesque, *Mol. Microbiol*., **47**, 1 (2003); https://doi.org/10.1046/j.1365-2958.2003.03289.x
15. V. Gaur and S. Bera, *Curr. Res. Pharmacol. Drug Discov*., **3**, 100137 (2022); https://doi.org/10.1016/j.crphar.2022.100137
16. H. Barreteau, A. Kovac, A. Boniface, M. Sova, S. Gobec and D. Blanot, *FEMS Microbiol. Rev*., **32**, 168 (2008); https://doi.org/10.1111/j.1574-6976.2008.00104.x
17. A.M. Kuttithodi, D. Nikhitha, J. Jacob, A. Narayanankutty, M. Mathews, O.J. Olatunji, R. Rajagopal, A. Alfarhan and D. Barcelo, *Molecules*, **27**, 8209 (2022); https://doi.org/10.3390/molecules27238209
18. A. Husain, A. Ahmad, I.A.I. Mkhalid, R. Mishra and M. Rashid, *Med. Chem. Res*., **22**, 1578 (2013); https://doi.org/10.1007/s00044-012-0137-4
19. S. Ammaji, S. Masthanamma, R R. Bhandare, S. Annadurai and A.B. Shaik, *Arab. J. Chem*., **15**, 103581 (2021); https://doi.org/10.1016/j.arabjc.2021.103581
20. P.S. Bhale, H.V. Chavan, R.S. Endait, A.T. Kadam, R.J. Bopalkar and M.S. Gaikwad, *Croat. Chem. Acta*, **94**, 35 (2021); https://doi.org/10.5562/cca3758
21. A.T. Bale, U. Salar, K.M. Khan, S. Chigurupati, T. Fasina, F. Ali, M. Ali, S.S. Nanda, M. Taha and S. Perveen, *Lett. Drug Design Discov*., **18**, 249 (2021); https://doi.org/10.2174/1570180817999201001155032
22. C.G.D. Raj, B.K. Sarojini, V. Bhanuprakash, R. Yogisharadhya, B.E.K. Swamy and R. Raghavendra, *Med. Chem. Res*., **21**, 2671 (2012); https://doi.org/10.1007/s00044-011-9793-z
23. A. Husain, M. Rashid, R. Mishra and D. Kumar, *Acta Pol. Pharm*., **70**, 443 (2013).
24. A.M. Asiri and S.A. Khan, *Molecules*, **16**, 523 (2011); https://doi.org/10.3390/molecules16010523
25. S. Burmaoglu, S. Ozcan, S. Balcioglu, M. Gencel, S.A.A. Noma, S. Essiz, B. Ates and O. Algul, *Bioorg. Chem*., **91**, 103149 (2019); https://doi.org/10.1016/j.bioorg.2019.103149
26. S. Ozcan, D.A. Anil, G.Y. Ozkat, F. Sanli, O. F. Karatas and S. Burmaoglu, *J. Mol. Struct*., **1329**, 141468 (2025); https://doi.org/10.1016/j.molstruc.2025.141468
27. A. Modzelewska, C. Pettit, G. Achanta, N.E. Davidson, P. Huang and S.R. Khan, *Bioorg. Med. Chem*., **14**, 3491 (2006); https://doi.org/10.1016/j.bmc.2006.01.003
28. U.K. Sharma, D. Mohanakrishnan, N. Sharma, D. Equbal, D. Sahal and A.K. Sinha, *Eur. J. Med. Chem*., **155**, 623 (2018); https://doi.org/10.1016/j.ejmech.2018.06.025
29. D. Olender, J. Kujawski, E. Baranowska-Wójcik, K. Sowa-Kasprzak, B. Skóra, A. Pawełczyk, L. Zaprutko, D. Szwajgier and K.A. Szychowski, *Heliyon*, **10**, e37147 (2024); https://doi.org/10.1016/j.heliyon.2024.e37147
30. R. Pereira, A.M.S. Silva, D. Ribeiro, V.L.M. Silva and E. Fernandes, *Eur. J. Med. Chem.*, **252**, 115280 (2023); https://doi.org/10.1016/j.ejmech.2023.115280
31. L. Siddiqui, M.B. Hawsawi, G.A. Chotana and R.S.Z. Saleem, *ACS Omega*, **9**, 42061 (2024); https://doi.org/10.1021/acsomega.4c04635
32. Q.M. Pham, T.H. Le, T.H. Pham, Q.T. Tran, T.L. Do, T.T.L. Vu and Q.L. Pham, *Vietnam J. Sci. Technol.*, **60**, 929 (2022); https://doi.org/10.15625/2525-2518/16459